BIOCHEMISTRY
including biophysical chemistry & molecular biology

Article

pubs.acs.org/biochemistry

NMR Studies of the Interaction between Human Programmed Cell Death 5 and Human p53

Hongwei Yao,[†,‡] Yingang Feng,[‡] Tao Zhou,[‡] Jinfeng Wang,*[,‡] and Zhi-Xin Wang[†,‡]

[†]MOE Key Laboratory of Bioinformatics, School of Life Sciences, Tsinghua University, Beijing 100084, China

[‡]National Laboratory of Biomacromolecules, Institute of Biophysics, Chinese Academy of Sciences, 15 Datun Road, Beijing 100101, China

Supporting Information

ABSTRACT: Human programmed cell death 5 (PDCD5) is a protein playing a significant role in regulating both the apoptotic and paraptotic cell deaths. Resent findings show that PDCD5 is a positive regulator of Tip60 and also has a potential ability to interact with p53. Here we aim to experimentally characterize the nature of the interactions between PDCD5 and the p53 N-terminal domain (NTD) and to depict the binding mode between two proteins. The interprotein binding interfaces were determined by NMR experiments performed with PDCD5 and various fragments of p53 NTD. The binding affinity was investigated using the NMR titration experiments. Analysis revealed that the PDCD5 binding site on p53 is localized within residues 41−56 of p53 TAD2 subdomain while p53 binds preferentially to the positively charged surface region around the C-terminals of helices α3 and α5 and the N-terminal of helix α4 of PDCD5. The binding is mainly mediated through electrostatic interactions. The present data suggested a model for the interaction between PDCD5 and the p53 NTD.

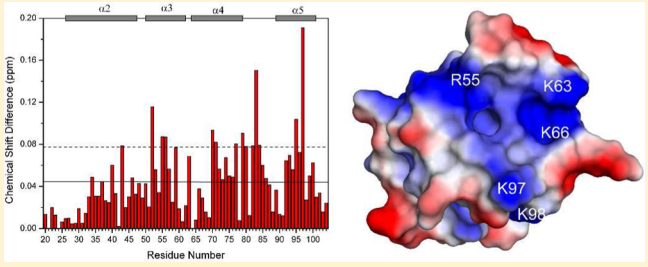

The gene of human programmed cell death 5 (PDCD5) encodes a protein expressed in tumor cells and translocated rapidly from the cytoplasm into the nuclei of cells during apoptosis independent of the apoptosis-inducing stimuli.[1,2] PDCD5 protein is an important regulator in both apoptotic and nonapoptotic programmed cell death.[3] The recombinant PDCD5 has a remarkable role in intercellular transport in various cells, serving as a vehicle having potential in the field of protein delivery to the cells. Studies by deletion mutagenesis indicated that PDCD5 can introduce the Mdm-2 binding domain of human p53 into living cells to induce cell death in human cancer cells.[4] Recently, it was found that PDCD5 can interact with Tip60, a histone acetyltransferases, and function as a coactivator to promote apoptosis via the Tip60-p53 signaling pathway. PDCD5 plays a positive role in Tip60-mediated p53 acetylation and p53-dependent proapoptotic gene expression. Interestingly, the GST pull-down assay has identified a potential ability of PDCD5 to physically interact with p53. These raise a possibility that PDCD5, Tip60, and p53 may form a ternary complex, and among them there may be an interregulatory network.[5]

The p53 protein is an important tumor suppressor, functioning by inducing apoptotic target genes to eliminate developing tumor cells. The basis for p53's apoptotic and tumor suppressive potency lies in its transcription-dependent and -independent functions.[6] In most human cancers, p53 is inactivated as a result of mutations in the p53 gene or as a result of alterations in genes whose products interact with p53 or transmit information to or from p53.[7] Recent research has confirmed that p53 can be activated by a variety of cellular stresses including DNA damage, oncogene activation, or hypoxia. After the activation, p53 can induce transcriptional activation of the apoptosis-related genes. Activation of p53 generated the subsequent biological outputs such as apoptosis, cell-cycle arrest, senescence, or modulation of autophagy.[8−10] The stress-induced p53 can translocate to mitochondria during p53-dependent apoptosis after DNA damage and hypoxia and can localize to the mitochondria outer membrane, inducing permeabilization of the outer mitochondrial membrane, which causes the release of potent death factors from the intermembraneous space into the cytosol, promoting apoptosis.[6,11] p53 is biologically active as a homotetramer comprising 4 × 393 amino acid residues, with each of its subunits having a modular structure. The natively unfolded N-terminal domain (NTD) contains a transactivation domain (TAD, residues 1−61) and a proline-rich region (PRR, residues 64−92). The TAD is further subdivided into the subdomains TAD1 (residues 1−40) and TAD2 (residues 40−61). The structured DNA-binding (DBD, residues 94−292) and tetramerization domains (TD, 324−355) are connected through a flexible linker region (residues 301−323). Similarly to the TAD region, the regulatory domain at the extreme carboxyl terminus (CTD, 360−393) is also intrinsically disordered.[12−16]

The 3D solution structure of human PDCD5 containing 125 amino acid residues has a compact core structure consisting of three helices α3, α4, and α5, forming a triple-helix bundle, and

Received: December 9, 2011
Revised: February 24, 2012
Published: February 28, 2012

dx.doi.org/10.1021/bi201822x | *Biochemistry* 2012, 51, 2684−2693

two terminal regions. The mobile N-terminal region comprises helices α1 and α2 while the flexible C-terminal region is unstructured.[17] Recent finding of the potential ability of PDCD5 to interact with p53 raised a question how PDCD5 interacts with p53. In order to address this question, various p53 fragments were obtained and used for determining the domain involved in the interaction with PDCD5. The protein−protein interaction studies using NMR method were carried out to further characterize and map the binding interfaces between two proteins. The results show that the PDCD5 binding site on p53 is localized within residues 41−56 of p53 TAD2 subdomain while p53 binds preferentially to the positively charged surface region around the C-terminals of helices α3 and α5 and the N-terminal of helix α4 of PDCD5. The possible binding mode is discussed.

MATERIALS AND METHODS

Protein Preparation. The PDCD5 and p53 fragments were used in the present study of the interaction between two proteins. The full-length PDCD5 and its fragment containing residues 20−104, namely PDCD5(20−104), were expressed and purified according to the procedures described previously.[17−19] The p53 fragments, namely p53(1−96), p53(1−73), p53(1−61), p53(1−40), p53(15−61), and p53(37−61), encoding residues 1−96, 1−73, 1−61, 1−40, 15−61, and 37−61, respectively, were amplified by PCR. Genes of these fragments were cloned into a modified version of pGBO expression vector,[20] in which an additional PreScission protease cleavage site was introduced between the His6-GB1 fusion partner and target proteins. The expression pGBO plasmids were transformed into *Escherichia coli* BL21(DE3) cells which were grown overnight in 20 mL LB medium at 37 °C. The overnight culture was used to inoculate another 1000 mL LB media (with 50 μg/mL kanamycin sulfate). Protein expression was induced with 1.0 mM isopropyl-D-thiogalactoside (IPTG) when the bacterial cells were grown to an A_{600} value of 0.8. After incubation for 4 h, the bacterial cells were collected by centrifugation at 4000 rpm for 30 min at 4 °C and stored at −20 °C. The cell pellets were lysed by sonication in buffer A (8 M urea or 6 M GdmCl, 25 mM Tris-HCl, pH 8.0, 150 mM NaCl). The clarified supernatant was loaded onto a Ni-NTA column pre-equilibrated with buffer A. The column was then washed with 6- to 10-column volumes of buffer A and 20 mM imidazole. Afterward, the column was washed with 10-column volumes of buffer B (25 mM Tris-HCl, pH 8.0, 150 mM NaCl). The protein was eluted from the column with 500 mM imidazole and was dialyzed against buffer B at 4 °C overnight. Then, the PreScission protease was added for cleavage of the fusion tag. The solution was concentrated to 1−2 mL and further purified using a Superdex 75 (Pharmacia) gel filtration column pre-equilibrated with 100 mM NH_4HCO_3. The purified protein was lyophilized and stored at −20 °C. The DNA fragment coding for p53(94−312) containing residues 94−312 was cloned into the NdeI and XhoI restriction sites of pET15b (Novagen). The p53(94−312) proteins were expressed and purified according to the procedures described in the early report.[21]

Three single-cysteine mutations, S15C, D61C, and M44C of p53(15−61) (which contains no cysteine in wild type), were constructed using site-directed mutagenesis for introduction of the nitroxide spin-label MTSL. The S15C, D61C, and M44C mutant p53(15−61), namely [S15C]p53(15−61), [D61C]-p53(15−61), and [M44C]p53(15−61), were expressed using the same protocol as described above. However, in the purification of mutant p53 fragments, the buffer for lysis of the cell pellets by sonication was changed to 8 M urea or 6 M GdmCl, 25 mM Tris-HCl, pH 8.0, 150 mM NaCl, 10 mM β-mercaptoethanol. After washing the column using buffer B, the spin-label reagent MTSL (Toronto Research Chemicals) used for attaching the nitroxide spin-label to the single-cysteine variants of mutant p53 fragments was added from a concentrated stock in acetonitrile at a molar ratio of 5:1 MTSL:protein and incubated at room temperature for more than 12 h. Excess MTSL reagent was washed out using buffer B. The spin-labeled mutant fragments were checked using MALDI-TOF mass spectrometry.

Uniformly ^{15}N- and/or ^{13}C-labeled proteins were obtained by growth in M9 minimal media containing $^{15}NH_4Cl$ and/or [^{13}C]-glucose as the sole nitrogen and/or carbon sources, respectively. The purity of proteins was checked by SDS-PAGE to ensure a single band.

NMR Spectroscopy. PDCD5 and its mixtures with p53 fragments used in the corresponding experiments were dissolved in 90% H_2O/10% D_2O containing 50 mM potassium phosphate buffer (pH 6.5), 200 mM NaCl, and 0.01% (w/v) sodium 2,2-dimethylsilapentane-5-sulfonate (DSS), whereas the samples for p53 fragments and their mixtures with PDCD5 contained 50 mM potassium phosphate buffer (pH 6.0), 100 mM KCl, and 0.01% (w/v) DSS. All NMR experiments were run on a Bruker DMX 600 spectrometer equipped with a triple-resonance cryo-probe. The 3D ^{1}H−^{13}C−^{15}N HNCACB, CBCA(CO)NH, HNCO, and HNCA and the 2D ^{1}H−^{15}N HSQC experiments were performed with p53 fragments at 298 K for assignment of backbone ^{1}H, ^{15}N, and ^{13}C resonances. The 2D ^{1}H−^{15}N HSQC experiments were adopted for investigation of the interaction between PDCD5 and p53 fragments. All NMR data were processed and analyzed using software FELIX 98.0 (Accelrys Inc.) and NMRView.[22] ^{1}H chemical shifts were referenced to internal DSS. ^{15}N and ^{13}C chemical shifts were referenced indirectly to DSS.[23]

Heteronuclear steady-state ^{1}H−^{15}N NOE was measured at 298 K for 0.46 mM p53(15−61) in the free state and for 0.46 mM p53(15−61) in the mixture with PDCD5(20−104) at PDCD5:p53(15−61) = 2.0 and 4.1 using standard pulse sequences. The proteins were dissolved in 92% H_2O/8% D_2O containing 50 mM potassium phosphate buffer (pH 6.0), 100 mM KCl, and 0.05 mM DSS, 0.02% (w/v) NaN_3, 1 mM EDTA, and 1/200 protease inhibitor (Novagen). The steady-state ^{1}H−^{15}N NOE spectra were acquired with and without ^{1}H saturation in an interleaved manner. The NOE values were calculated from the ratios of the peak intensities with and without proton saturation.

In order to identify residues in PDCD5(20−104) affected by the interaction of spin-labeled [S15C]p53(15−61), [D61C]-p53(15−61), and [M44C]p53(15−61), the 2D ^{1}H−^{15}N HSQC spectra of the ^{15}N-labeled PDCD5(20−104) were recorded at 298 K in the presence of spin-labeled p53 fragments. All experiments were repeated after the spin-label was reduced with 10-fold excess ascorbic acid. The NMR samples were prepared by mixing of 0.3 mM ^{15}N-labeled PDCD5(20−104) with nitroxide spin-labeled [S15C]p53(15−61), [D61C]p53(15−61), and [M44C]-p53(15−61) at a molar ratio of 1:1. To ensure complete reduction of the spin-label, the samples containing ascorbic acid were placed at room temperature for 1 h.

NMR Titration Experiments. Titration of PDCD5(20−104) with p53(15−61) and reverse titration were monitored by 2D ^{1}H−^{15}N HSQC spectra of titrated PDCD5(20−104) and p53(15−61) at 308 and 298 K, respectively. The 2D ^{1}H−^{15}N HSQC spectra of 0.3 mM ^{15}N-labeled PDCD5(20−104) were

dx.doi.org/10.1021/bi201822x | *Biochemistry* 2012, 51, 2684−2693

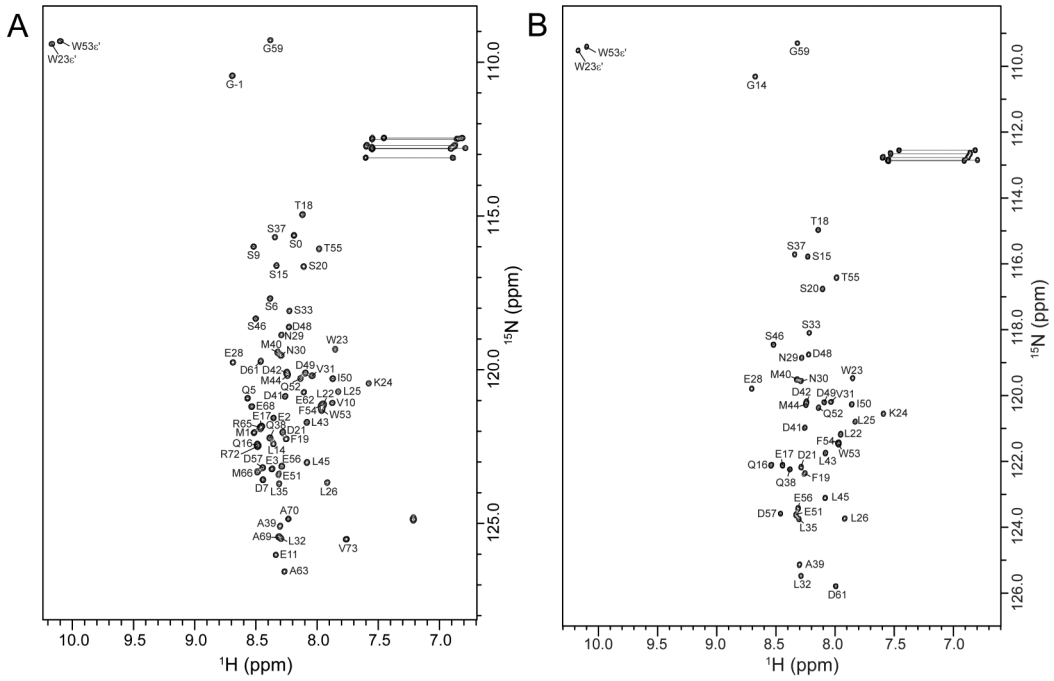

Figure 1. Residue-specific assignments for backbone amide groups of p53 fragments. The assignments of cross-peaks are given by one-letter amino acid code and the sequence positions in the corresponding 2D ^{1}H−^{15}N HSQC spectra obtained at 298 K and pH 6.0. A prime mark denotes folded cross-peaks. (A) The assignments for 60 residues of p53(1−73), except 13 prolines. Cross-peaks labeled as G-1 and S0 are from glycine and serine in the tag residues GPGS appended to residue M1 in p53(1−73) sequence resulting from fusion tag cleavage by PreScission protease digestion. (B) Assignments for 41 residues of p53(15−61), except 6 prolines. Cross-peaks labeled as G14 is the tag residue appended to residue S15. (C) The sequence of p53(1−73).

acquired with increased amount of unlabeled p53(15−61) at p53(15−61):PDCD5(20−104) molar ratio of 0, 0.25, 0.5, 0.73, 1.0, 1.22, 1.46, 1.9, 2.9, and 3.9. In the reverse titration experiments, the concentration of ^{15}N-labeled p53(15−61) was fixed at 0.46 mM, and 2D ^{1}H−^{15}N HSQC spectra of p53(15−61) were recorded at PDCD5(20−104):p53(15−61) molar ratio of 0, 0.125, 0.27, 0.5, 0.77, 1.0, 1.5, 2.0, 2.5, 3.1, 3.6, and 4.1. The observed chemical shift changes in the titration experiments were calculated according to the equation

$$\Delta_{obs} = \{0.5[(\delta_{H,bound} - \delta_{H,free})^2 + 0.04(\delta_{N,bound} - \delta_{N,free})^2]\}^{1/2}$$

where $\delta_{H,bound}$ and $\delta_{N,bound}$ are the chemical shifts of amide ^{1}H and ^{15}N resonances, respectively, at a bound state, whereas $\delta_{H,free}$ and $\delta_{N,free}$ are those at a free state of the protein. Based on the PDCD5(20−104):p53(15−61) = 1:1 binding mode, the dissociation constant K_d was obtained by fitting the observed chemical shift changes to the equation[24]

$$\Delta_{obs} = 0.5\Delta_{max} \times \{(1 + X + K_d/[P]_0) - [(1 + X + K_d/[P]_0)^2 - 4X]^{1/2}\}$$

where Δ_{obs} is the observed chemical shift change at any arbitrary equilibrium state, Δ_{max} is the chemical shift change at a fully bound state, X is the molar ratio of ligand to protein, and $[P]_0$ is the initial concentration of protein.

RESULTS

Resonance Assignments for p53 Fragments. It was proposed that the lack of a rigid structure of p53 may allow its physiological interaction with a multitude of partner proteins and the regulation of its turnover.[15] The entire N-terminal domain (NTD) of p53 (residues 1−93) containing an acidic transactivation domain (TAD) and a proline-rich domain is natively unfolded under physiological conditions since it is devoid of tertiary structure and largely missing secondary structure elements.[16] The TAD domain was found to be required for interaction with components of the transcriptional machinery.[25] The present study adopted the NTD domain of p53 to explore the interaction between PDCD5 and p53 by NMR spectroscopy. A series of fragments of p53 NTD domain were obtained to identify the sites for interacting with PDCD5. Among them fragment p53(1−73) was subjected to the 3D heteronuclear NMR studies for obtaining the residue-specific assignment.

The fragment p53(1−73) contains two subdomains (TAD1 and TAD2) of the p53 TAD domain. Figure 1A shows the resonance assignments for backbone nitrogen and amide protons of p53(1−73). All of the cross-peaks for 60 residues of p53(1−73) in the 2D ^{1}H−^{15}N HSQC spectrum were identified

dx.doi.org/10.1021/bi201822x | Biochemistry 2012, 51, 2684−2693

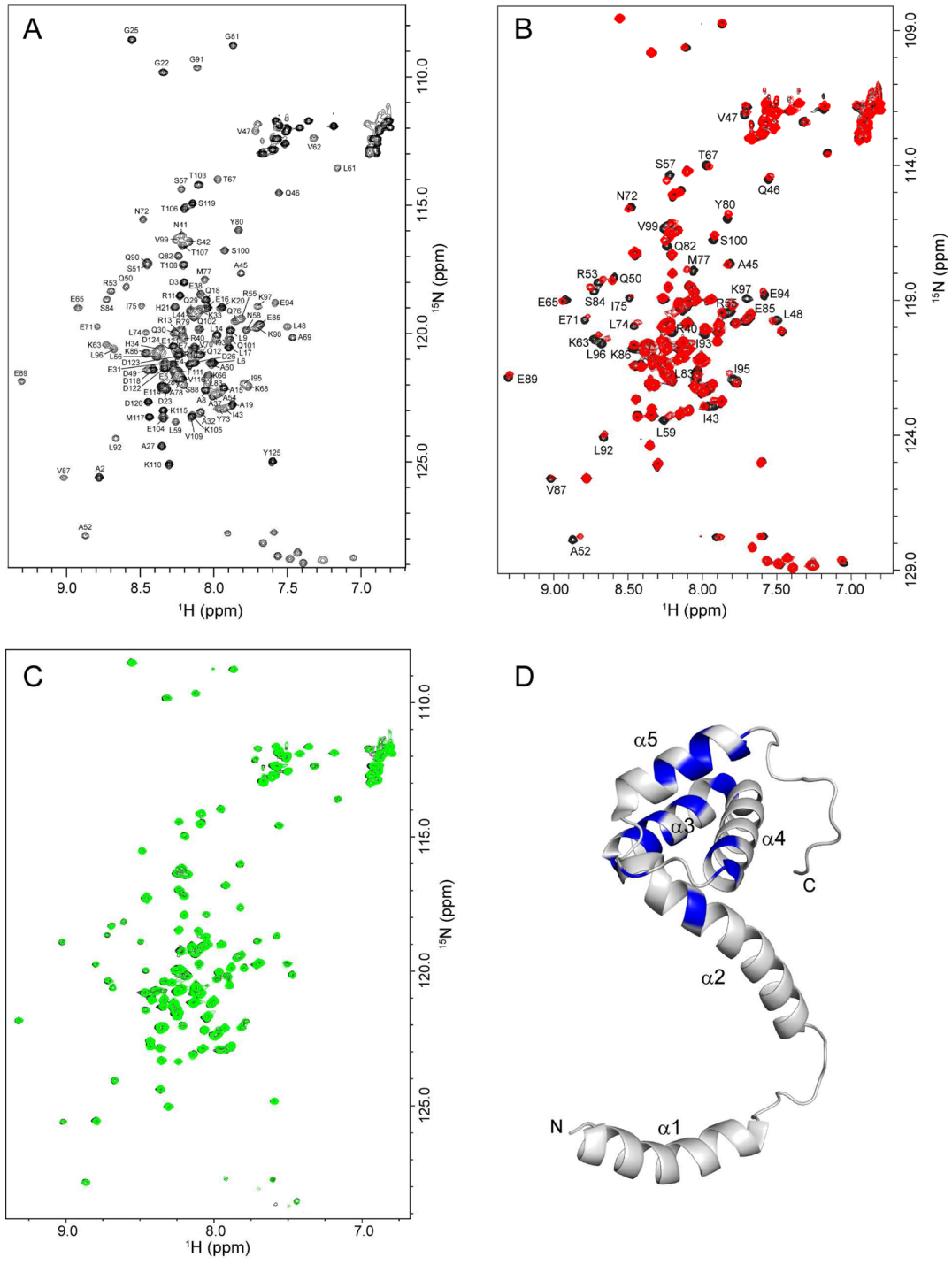

Figure 2. Detecting the binding site of p53(1−96) on PDCD5. (A) 2D ^{1}H−^{15}N HSQC spectrum of full-length PDCD5 showing the residue-specific assignments of backbone amide groups. The assigned cross-peaks are indicated by labeling the one-letter amino acid code and residue number. (B) 2D ^{1}H−^{15}N HSQC spectrum of 0.2 mM ^{15}N-labeled PDCD5 (black) is overlaid with the spectrum recorded for ^{15}N-labeled PDCD5 mixed with unlabeled p53(1−96) in 1:1 molar ratio (red). (C) Overlay of the 2D HSQC spectra of ^{15}N-labeled PDCD5 in mixture with unlabeled p53(94−312) (green) and free ^{15}N-labeled PDCD5 (black). (D) Mapping of the p53(1−96) binding surface on the PDCD5 structure (PDB ID 2K6B). Residues with significant chemical shift differences are shown in blue.

except 13 prolines. The resonances of amide protons for 60 cross-peaks crowded a narrow range of 7.6−8.7 ppm in the spectrum, indicating a largely unfolded conformation of the fragment p53(1−73), which was consist with the secondary structure analysis with TALOS+ (Figure S1 in the Supporting Information). Figure 1B shows the 2D ^{1}H−^{15}N HSQC spectrum of p53(15−61), a p53 fragment chosen for extensive studies in the present work (see below). The resonance signals of almost all the cross peaks in the spectrum of p53(15−61) show very similar chemical shifts to those of the corresponding cross-peaks in the spectrum of p53(1−73), except two terminal residues S15 and D61. Resonance assignments for residues of p53(15−61) were achieved simply following the assignments of resonances in the spectrum of p53(1−73).

dx.doi.org/10.1021/bi201822x | *Biochemistry* 2012, 51, 2684−2693

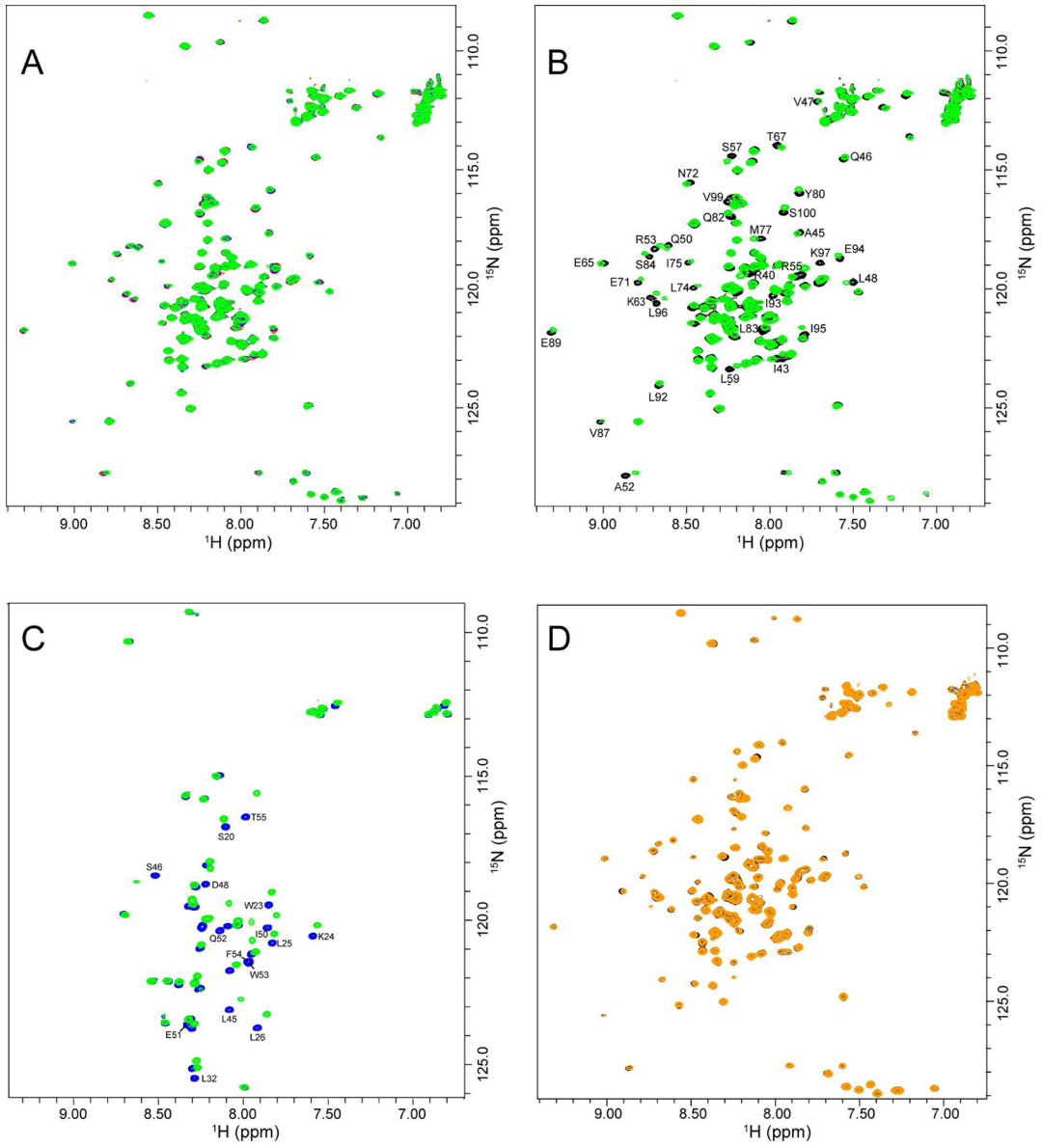

Figure 3. 2D ^{1}H−^{15}N HSQC spectra of the mixtures of PDCD5 and different p53 fragments. (A) Overlay of the spectra of ^{15}N-labeled PDCD5 in the mixtures with unlabeled p53(1−73) (red), p53(1−61) (blue), and p53(15−61) (green). (B) Overlay of the spectra of ^{15}N-labeled PDCD5 in mixture with unlabeled p53(15−61) (green) and free ^{15}N-labeled PDCD5 (black). (C) Overlay of the spectra of ^{15}N-labeled p53(15−61) in mixture with unlabeled PDCD5 (green) and free ^{15}N-labeled p53(15−61) (blue). (D) Overlay of the spectra of ^{15}N-labeled PDCD5 in mixture with unlabeled p53(1−40) (orange) and free ^{15}N-labeled PDCD5 (black). All the mixtures of PDCD5 with p53 fragments were prepared in 1:1 molar ratio except the mixture of PDCD5 and p53(1−40).

Interaction between PDCD5 and p53 Proteins. For detecting the interaction surfaces between p53 and PDCD5, the fragments p53(1−96) containing entire NTD domain and p53(94−312) consisting of a structured DBD domain were adopted for preparing the mixture samples with PDCD5. The 2D ^{1}H−^{15}N HSQC spectra of ^{15}N-labeled full-length PDCD5 in the mixtures with p53(1−96) and p53(94−312), respectively, were obtained, which were compared to the 2D HSQC spectrum of free PDCD5 (Figure 2). The resonance assignments for backbone amide groups of full-length PDCD5 (Figure 2A) were quoted from the previous study.[17] Figure 2B shows shifting of resonance signals for a number of residues of PDCD5 while interacting with p53(1−96). Relatively significant changes in chemical shifts of $^{1}H_N$ and ^{15}N resonances were observed for residues Q50, A52, R53, R55, S57, and L59 in the helix α3 (residues 50−62); M77 in the C-terminal region of helix α4 (residues 64−79); I93, I95, L96, K97, V99, and S100 in the helix α5 (residues 89−101); Y80 and S84 in the loop $L_{\alpha4\alpha5}$ between helices α4 and α5 and K63 linking helices α3 and α4; and residue I43 in the C-terminal region of helix α2 (residues 26−47) according to the 3D solution structure of PDCD5 (PDB ID 2K6B).[17] Apparently, p53(1−96) interacts mainly with the core structural region of PDCD5 (Figure 2D). Nevertheless, fragment p53(94−312) did not interact with PDCD5, and no resonance shifting can be observed in the 2D ^{1}H−^{15}N HSQC spectrum of PDCD5 mixed with p53(94−312) (Figure 2C). Therefore, the interaction of PDCD5 with p53 mainly occurs to the core structure of PDCD5 and NTD domain of p53.

dx.doi.org/10.1021/bi201822x | *Biochemistry* 2012, 51, 2684−2693

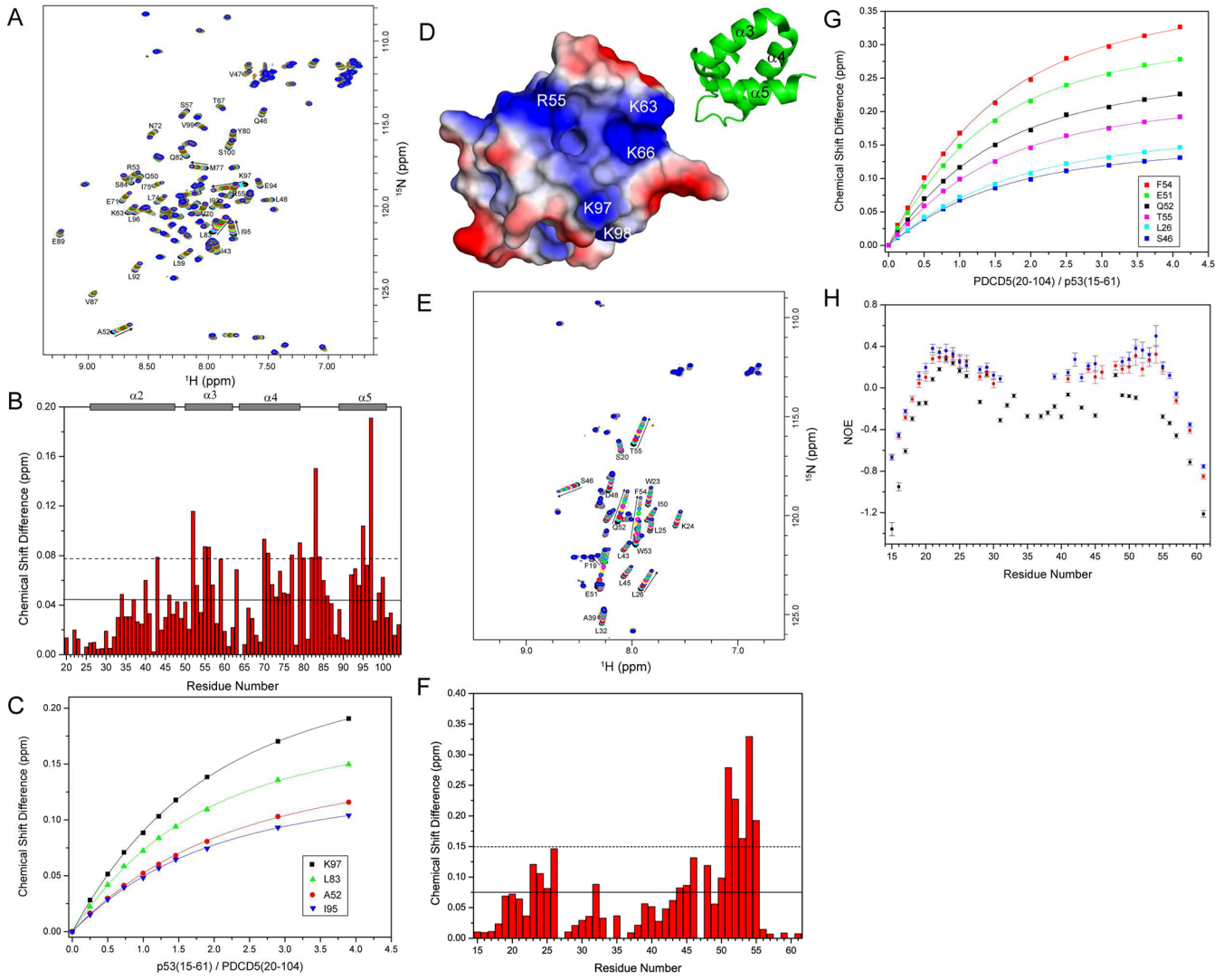

Figure 4. Titration of p53(15−61) and PDCD5(20−104) by monitoring the chemical shift changes of resonance signals in the 2D ^{1}H−^{15}N HSQC spectra of PDCD5(20−104) and p53(15−61), respectively. (A) Spectrum of PDCD5(20−104) combined together the spectra recorded at various p53(15−61) concentrations. (B) Weighted chemical shift differences ($\Delta\delta$) between resonances for PDCD5(20−104) in the presence of p53(15−61) at p53(15−61):PDCD5(20−104) = 3.9 and those in the absence of p53(15−61). Solid and dashed horizontal lines correspond to the average chemical shift change and one standard deviation above the average, respectively. (C) Chemical shift changes for A52, L83, I95, and K97 as a function of p53(15−61) concentration in the titration experiments. The solid curves are the curve fitting results from the 1:1 binding mode. (D) Molecular surface of PDCD5 colored by electrostatic potential (blue, positively charged; red, negatively charged; white, neutral). The positively charged residues on the molecular surface are labeled. Only the core structural region (R40-Q101) of PDCD5 is shown. (E) Spectrum of p53(15−61) combined together the spectra recorded at various PDCD5(20−104) concentrations. (F) Weighted chemical shift differences ($\Delta\delta$) between resonances for p53(15−61) in the presence of PDCD5(20−104) at PDCD5(20−104):p53(15−61) = 4.1 and those in the absence of PDCD5(20−104). Solid and dashed horizontal lines correspond to the average chemical shift change and one standard deviation above the average, respectively. (G) Chemical shift changes for L26, S46, E51, Q52, F54, and T55 as a function of PDCD5(20−104) concentration in the titration experiments. The solid curves are the curve fitting results from the 1:1 binding mode. (H) Heteronuclear steady-state ^{1}H−^{15}N NOE values as a function of sequence for p53(15−61) in the free state (black) and in the mixture with PDCD5(20−104) at molar ratio of PDCD5(20−104):p53(15−61) = 2 (red) and 4.1 (blue).

To detect which region in the NTD domain of p53 is responsible for interacting with PDCD5, fragments p53(1−40), p53(1−61), p53(1−73), and p53(15−61) were added into the ^{15}N-labeled full-length PDCD5 sample solution making the corresponding mixture samples. 2D ^{1}H−^{15}N HSQC spectrum was recorded for each of these mixture samples. The 2D HSQC spectra of PDCD5 mixed with p53(1−61), p53(1−73), and p53(15−61) were essentially identical (Figure 3A). Of them, the 2D HSQC spectrum of PDCD5 mixed with p53(15−61) (Figure 3B) showed the resonance shifting similar to that of PDCD5 mixed with p53(1−96) (Figure 2B). This indicated that two subdomains, TAD1 and TAD2, in the NTD domain of p53 may be involved in the interaction with PDCD5. On the other hand, the 2D HSQC spectrum of p53(15−61) in the mixture with PDCD5 (Figure 3C) showed resonance shifting of the cross peaks for residues S20, W23, K24, L25, L26, L32, L45, S46, D48, I50, E51, Q52, W53, F54, and T55 of p53(15−61). Of them, the former six residues are in the C-terminal portion of TAD1 subdomain and the rest residues are in the TAD2 subdomain. The same resonance shifting was observed in the spectrum recorded for p53(1−73) mixed with PDCD5 (Figure S2 in the Supporting Information). Therefore, the

dx.doi.org/10.1021/bi201822x | *Biochemistry* 2012, 51, 2684−2693

TAD2 subdomain and the C-terminal portion of TAD1 subdomain of p53 NTD domain should be involved in the interaction with PDCD5, and p53(15−61) is a fragment which happens to cover these sequence regions. However, p53(1−40), a fragment containing only TAD1 subdomain, provided a 2D HSQC spectrum showing very slightly chemical shift changes of a few cross-peaks (Figure 3D). This implies that the TAD2 subdomain may be a region in p53 NTD domain responsible for interacting with PDCD5.

Characterizing the Binding of PDCD5 with p53 Fragment. In order to characterize the binding features of PDCD5 and p53 fragments, the PDCD5(20−104) and p53(15−61) were adopted in the titration experiments for facilitating the spectral analysis by reducing the cross-peak crowding in the 2D $^{1}H-^{15}N$ HSQC spectra. The 2D $^{1}H-^{15}N$ HSQC spectrum of ^{15}N-labeled p53(15−61) mixed with PDCD5(20−104) (spectrum not shown) was very similar to that of ^{15}N-labeled p53(15−61) mixed with full-length PDCD5 because the N-terminal helix α1 (residues 2−17) and C-terminal loop (residues 102−125) of PDCD5 was not involved in the interaction with p53 fragments. A series of 2D $^{1}H-^{15}N$ HSQC spectra of ^{15}N-labeled PDCD5(20−104) and p53(15−61) were recorded in the presence of increased amounts of unlabeled p53(15−61) and PDCD5(20−104), respectively. In the titration of PDCD5-(20−104) with p53(15−61), the 2D HSQC spectra of PDCD5(20−104) showed shifting of resonance signals for a number of residues as the concentration of p53(15−61) increased (Figure 4A). Relatively significant changes in chemical shifts of $^{1}H_N$ and ^{15}N resonances were observed for residues A52, R55, L56, V70, E71, M77, R79, L83, I95, and K97 (Figure 4B). The dissociation constant K_d of p53(15−61) with PDCD5(20−104) was obtained by fitting the chemical shift changes of amide group resonances for residues A52, L83, I95, and K97 (Figure 4C), assuming a single binding mode. Averaging the K_d values obtained for these four residues gave a value of 410 ± 59 μM. On the other hand, titration of p53(15−61) with PDCD5(20−104) caused the significant chemical shift changes for residues W23, K24, L26, S46, D48, E51, Q52, W53, F54, and T55 of p53(15−61) (Figure 4E,F). Fitting the chemical shift changes of amide resonances for residues L26, S46, E51, Q52, F54, and T55 of p53(15−61) (Figure 4G) gave an average K_d value of 412 ± 52 μM, which is in close proximity to that obtained by titration of PDCD5(20−104) with p53(15−61). The isothermal titration calorimetry (ITC) studies using the same p53 fragment and PDCD5 protein as in the NMR titration experiments gave a K_d value of 138 ± 18 μM for binding of p53(15−61) with PDCD5(20−104) (Figure S3 in the Supporting Information). Therefore, the binding between p53 and PDCD5 was not very tight and was on the fast-exchange time scale relative to the resonance frequency differences between the free and bound proteins since both titration induced continuous movements of specific cross-peaks in the corresponding 2D HSQC spectra.

Because the entire N-terminal part of p53 (1−93) is natively unfolded under physiological conditions,[16] p53(15−61) is natively unfolded with flexible backbone. To examine changes in the backbone flexibility of p53(15−61) while bound to PDCD5, the heteronuclear steady-state $^{1}H-^{15}N$ NOE values were obtained for p53(15−61) and for its mixtures with PDCD5(20−104) (Figure 4H). Majority residues in p53(15−61) have NOE values below zero except residues 21−26 having NOE values >0. However, binding of PDCD5 caused an increase in $^{1}H-^{15}N$ NOE values of residues 19−31 and 39−56 of p53(15−61). Especially, the NOE values for residues 41−56 increased largely from the values below zero to the values around 0.2 under the interaction of PDCD5. Therefore, restriction of the local motions of residues 41−56 is increased while PDCD5 binds to p53(15−61), although the entire fragment of p53(15−61) is still highly flexible with $^{1}H-^{15}N$ NOE values <0.6.

DISCUSSION

Preferential Binding Sites on p53(15−61) and PDCD5(20−104). The fragment p53(1−73) contains two contiguous subdomains (TAD1 and TAD2) of the natively unfolded acidic transcriptional activation domain (TAD). An NMR study of p53(1−73) fragment at 5 °C has revealed that an amphipathic helix (residues 18−26 of TAD1 subdomain) and two nascent turns (residues 40−44 and 47−53 of TAD2 subdomain) populated in the fragment while there is no ordered structure formation.[26] Fragment p53(15−61) happens to cover these sequence regions, which means natively unfolded p53(15−61) can be populated such local secondary structures. According to the chemical shift changes (Figure 3C), it seems residues S20, W23, K24, L25, and L26 in the amphipathic helix and residues L45, S46, D48, I50, E51, Q52, W53, F54, and T55 in the extended second nascent turn of p53(15−61) are involved in the interaction with PDCD5. However, the relatively large chemical shift changes of resonance signals were observed for residues in the region around second nascent turn in comparison with that in the region of amphipathic helix of p53(15−61) (Figure 4F). Besides, the 2D $^{1}H-^{15}N$ HSQC spectrum of fragment p53(37−61) (Figure S4 in the Supporting Information), but not the spectrum of p53(1−40) (Figure 3D), showed large shifting of resonance signals under the interactions of PDCD5. Therefore, the TAD1 subdomain of p53 along has no significant interaction with PDCD5, and the TAD2 subdomain is a main region responsible for interacting with PDCD5. The TAD2 subdomain contains sequence region 41−56 which has conformation of two nascent turns. The heteronuclear $^{1}H-^{15}N$ NOE measurements for p53(15−61) in the absence and presence of PDCD5(20−104) indicated that binding of PDCD5(20−104) to p53(15−61) largely influenced the backbone local motions of the residues 41−56 but not the residues in the region around amphipathic helix of p53(15−61) (Figure 4H). This suggested strongly that residues 41−56 of TAD2 subdomain form a preferential binding site for PDCD5(20−104) on p53(15−61).

The sequence of p53(15−61) contains 11 negatively charged residues, of them six (D41, D42, D48, D49, E51, and E56) are located in the sequence region 41−56 (Figure 1C). Therefore, the PDCD5(20−104) binding site on p53(15−61) is a highly anionic moiety since no any positively charged residue is in this region. On the other hand, 15 positively charged residues in PDCD5(20−104) distributed mainly in the core structural region. Residues K33, H34, R35, and R40 are in the helix α2; helix α3 has residues R53 and R55 including K63 linked to its C-terminal end; residues K66, K68, and R79 are located in the helix α4; residues K97 and K98 are in the helix α5; and K86 is in the loop $L_{\alpha4\alpha5}$. The other two are at the N-terminal end of PDCD5(20−104).[17] According to the 3D solution structure of PDCD5, helix α2 of PDCD5 has a mobile N-terminal part (26−43) and a less mobile C-terminal portion (44−47). Among the positively charged residues only the residues R55 and K63 in the structural region of helix α3; K66 in the helix α4; and K97 and K98 in the helix α5 can create a positively charged surface on PDCD5(20−104) (Figure 4D), showing a relatively high

concentration of positive charge at a surface region around the C-terminals of helices α3 and α5 and the N-terminal of helix α4. It seems this positively charged surface region on PDCD5(20−104) can preferentially recognize the anionic moiety of p53(15−61). Besides, the most strong chemical shift perturbation was observed for the bulk of residues over the helices α3, α4, and α5 of PDCD5 while binding to p53(15−61) (Figures 2B and 4B). Therefore, the binding of PDCD5(20−104) with p53(15−61) may occur between residues 41−56 of p53(15−61) and the positively charged surface region of PDCD5(20−104). Presumably, the electrostatic interactions mediated predominantly the binding between two proteins.

The Possible Mode of Binding. The weak binding of p53(15−61) with PDCD5(20−104), having a K_d of 412 μM, was on the fast-exchange between free and bound states. Besides, p53(15−61) is a natively disordered fragment. Therefore, it was unable to obtain the intermolecular NOE data for structural analysis using NMR technique. To further map the binding site for p53(15−61) on PDCD5(20−104), paramagnetic relaxation was adopted since the magnitude of the paramagnetic relaxation enhancement (PRE) is proportional to the $\langle r^{-6} \rangle$ average distance between a proton and a paramagnetic center, and the effect of the spin-labels can be observed up to 20 Å from the paramagnetic center.[27] The PRE effect is reflected by the ratios of cross-peak heights between oxidized and reduced spectra (I_{ox}/I_{red}). The pronounced minima in the PRE profiles of PDCD5(20−104) under the interactions of p53(15−61) with the N- and C-terminal spin probes from [S15C]p53(15−61) and [D61C]p53(15−61), respectively, and with the middle-region spin probe from [M44C]p53(15−61) were revealed in Figure 5. Figure 5A,B shows that the amide protons of residues in the C-terminal portions of helices α2 and α4 and the loop $L_{\alpha4\alpha5}$ of PDCD5(20−104) were affected significantly by the spin-labels. Besides, the relatively weak PRE effect was seen on the N-terminal of helix α4 and the C-terminal portions of helices α3 and α5. In addition, the PRE effect on PDCD5(20−104) by the N-terminal spin probe from [S15C]p53(15−61) was much stronger than that by the C-terminal spin probe from [D61C]p53(15−61). However, the relatively stronger PRE effect on the C-terminal portions of helices α3 and α5 and the N-terminal of helix α4 of PDCD5(20−104) under the interaction of [M44C]p53(15−61) was observed in Figure 5C as compared with Figure 5A,B.

The above-described PRE effect on PDCD5(20−104) may depict a possible binding mode between p53(15−61) and PDCD5-(20−104). In the binding of p53(15−61) with PDCD5(20−104), the segment 41−56 containing residues D41, D42, D48, D49, E51, and E56 of p53(15−61) preferentially binds to the positively charged surface region formed by residues R55, K63, K66, K97, and K98 in the C-terminal portions of helices α3 and α5 and the N-terminal of helix α4 of PDCD5(20−104). The interprotein orientation of p53(15−61) to PDCD5(20−104) could be alternative due to the nonspecific binding. In such binding mode, the N- and C-terminal spin probes of p53(15−61) cannot affect the residues in the binding surface of PDCD5(20−104). However, the long N-terminal portion (15−40) of p53(15−61) presumably has the superiority over the short C-terminal portion (57−61) to contact with loop $L_{\alpha4\alpha5}$ and the C-terminal portions of helix α4 and α2 according to the 3D structure of PDCD5. Thus, statistically, the N-terminal spin probe from [S15C]p53(15−61) has more significant PRE effect on the corresponding parts of PDCD5 (Figure 5B) than the C-terminal spin probe from [D61C]p53(15−61) (Figure 5A). Nevertheless, the M44C spin probe is in the segment D41-E56 of p53(15−61). The anionic moiety of residues

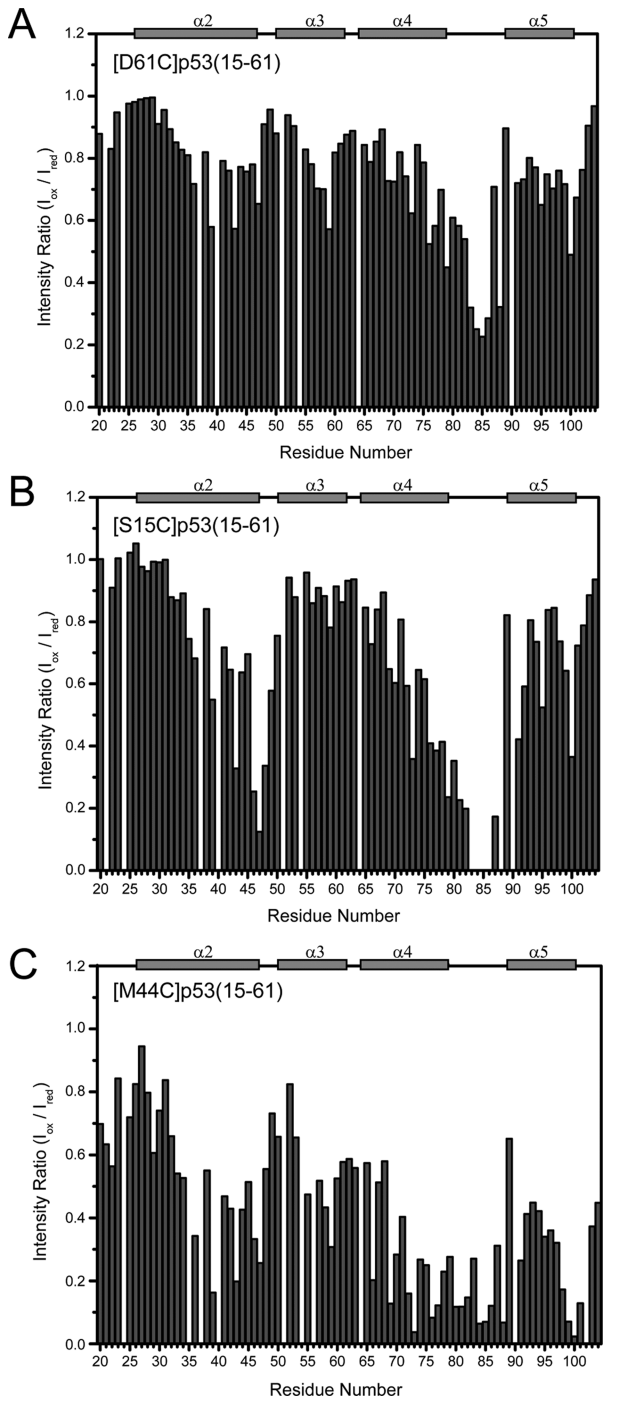

Figure 5. Bar graphs of intensity ratios of backbone amide protons versus primary sequence for PDCD5(20−104) in mixture with spin-labeled p53(15−61) at single-cysteine mutant positions D61C (A), S15C (B), and M44C (C). The 2D $^1H-^{15}N$ HSQC spectra of PDCD5(20−104) in the presence of spin-labeled p53(15−61) before (paramagnetic) and after (diamagnetic) reduction of the spin-label with ascorbate were recorded and the intensity ratios of the backbone amide signals between oxidized (I_{ox}) (paramagnetic) and reduced (I_{red}) (diamagnetic) spectra (I_{ox}/I_{red}) was determined. Blank spaces in the diagrams are either due to proline residues (position 24 and 64) or the inability to measure the peak height as a consequence of overlapping or nonassigned residues.

D41-E56 drives the binding of p53(15−61) to the positively charged surface region of PDCD5(20−104); thus, M44C spin probe generates relatively strong PRE effects on the residues in the

dx.doi.org/10.1021/bi201822x | Biochemistry 2012, 51, 2684−2693

C-terminals of helices α5 and α3 and the N-terminal of helix α4 of PDCD5. Since the effect of the spin-label can be observed up to 20 Å from the M44C, residues in the locations other than the binding surface of PDCD5 can be affected also by M44C as shown in Figure 5C. However, for further clarifying the binding between PDCD5 and p53(15−61), three-dimensional binding mode will be interested.

As is known, both PDCD5 and p53 are apoptosis-related proteins. PDCD5 translocated to cellular nucleus during apoptosis.[1] p53 can be activated in response to DNA damage and other cellular stresses, which was found to trigger apoptosis even in the absence of nucleus.[28] The K120 acetylation of p53 is induced by DNA damage and may have a decisive function in determining the outcome of p53 apoptosis induction.[29] PDCD5 could enhance the acetylation of p53 at K120 and is required for cell apoptosis induced by DNA damage.[5] Nevertheless, the present NMR study reveals that PDCD5 can interact with p53 NTD but not p53 DBD which contains the acetylation site K120 of p53. According to the reports, Tip60 is required for the acetylation of the endogenous p53 protein at K120, and PDCD5 binds to Tip60 and increases Tip60-dependent K120 acetylation of p53 (5). From these results, it can be postulated that PDCD5 may interact simultaneously with acetyltransferase domain of Tip60 and p53 NTD and facilitate the acetylation of p53 at K120 in the DNA binding domain. As a consequence, the results of present study on interaction between PDCD5 and p53 may provide some positive information for further investigation of apoptosis mechanism of PDCD5.

■ ASSOCIATED CONTENT

Ⓢ Supporting Information

Secondary structure analysis with TALOS+ showing the unfolding of the purified p53(1−73) (Figure S1); 2D $^{1}H-^{15}N$ HSQC spectrum of p53(1−73) in the mixture with PDCD5 (Figure S2); ITC measurements for detecting the interaction of PDCD5(20−104) with p53 TAD domain (Figure S3); 2D $^{1}H-^{15}N$ HSQC spectra of p53(37−61) titrated with PDCD5(20−104) (Figure S4). This material is available free of charge via the Internet at http://pubs.acs.org.

■ AUTHOR INFORMATION

Corresponding Author

*Tel: +86 10 64888498; Fax: +86 10 64872026; e-mail: jfw@sun5.ibp.ac.cn.

Funding

This work was supported by grants from the National Natural Science Foundation of China (NNSFC) 30170201 and 30770434 (to J.W.), the NNSFC 30800179 and the Beijing Natural Science Foundation 5092018 (to Y.F.), and the China Postdoctoral Science Foundation 20090460350 (to H.Y.).

Notes

The authors declare no competing financial interest.

■ ABBREVIATIONS

PDCD5, programmed cell death 5; NTD, N-terminal domain; TAD, transactivation domain; PRR, proline-rich region; DBD, DNA-binding domain; TD, tetramerization domain; CTD, carboxyl terminus domain; IPTG, isopropyl-D-thiogalactoside; MTSL, (1-oxyl-2,2,5,5-tetramethyl-Δ^3-pyrroline-3-methyl)-methanethiosulfonate; DSS, 2,2-dimethyl-2-silapentane-5-sulfonate; PRE, paramagnetic relaxation enhancement.

■ REFERENCES

(1) Chen, Y. Y., Sun, R. H., Han, W. L., Zhang, Y. M., Song, Q. S., Di, C. H., and Ma, D. L. (2001) Nuclear translocation of PDCD5 (TFAR19): an early signal for apoptosis? *FEBS Lett. 509*, 191−196.

(2) Rui, M., Chen, Y. Y., Zhang, Y. M., and Ma, D. L. (2002) Transfer of anti-TFAR19 monoclonal antibody into HeLa cells by in situ electroporation can inhibit the apoptosis. *Life Sci. 71*, 1771−1778.

(3) Wang, Y., Li, X. T., Wang, L., Ding, P. G., Zhang, Y. M., Han, W. L., and Ma, D. L. (2004) An alternative form of paraptosis-like cell death, triggered by TAJ/TROY and enhanced by PDCD5 over-expression. *J. Cell Sci. 117*, 1525−1532.

(4) Wang, Y., Li, D., Fan, H., Tian, L. J., Zhong, Y. C., Zhang, Y. M., Yuan, L., Jin, C. N., Yin, C. H., and Ma, D. L. (2006) Cellular uptake of exogenous human PDCD5 protein. *J. Biol. Chem. 281*, 24803−24817.

(5) Xu, L. J., Chen, Y. Y., Song, Q. S., Xu, D., Wang, Y., and Ma, D. L. (2009) PDCD5 interacts with Tip60 and functions as a cooperator in acetyltransferase activity and DNA damage-induced apoptosis. *Neoplasia 11*, 345−U346.

(6) Mihara, M., Erster, S., Zaika, A., Petrenko, O., Chittenden, T., Pancoska, P., and Moll, U. M. (2003) p53 has a direct apoptogenic role at the mitochondria. *Mol. Cell 11*, 577−590.

(7) Vogelstein, B., Lane, D., and Levine, A. J. (2000) Surfing the p53 network. *Nature 408*, 307−310.

(8) Yee, K. S., and Vousden, K. H. (2005) Complicating the complexity of p53. *Carcinogenesis 26*, 1317−1322.

(9) Riley, T., Sontag, E., Chen, P., and Levine, A. (2008) Transcriptional control of human p53-regulated genes. *Nat. Rev. Mol. Cell Biol. 9*, 402−412.

(10) Green, D. R., and Kroemer, G. (2009) Cytoplasmic functions of the tumour suppressor p53. *Nature 458*, 1127−1130.

(11) Green, D. R., and Evan, G. I. (2002) A matter of life and death. *Cancer Cell 1*, 19−30.

(12) Chang, J., Kim, D. H., Lee, S. W., Choi, K. Y., and Sung, Y. C. (1995) Transactivation ability of p53 transcriptional activation domain is directly related to the binding-affinity to TATA-binding protein. *J. Biol. Chem. 270*, 25014−25019.

(13) Walker, K. K., and Levine, A. J. (1996) Identification of a novel p53 functional domain that is necessary for efficient growth suppression. *Proc. Natl. Acad. Sci. U. S. A. 93*, 15335−15340.

(14) Joerger, A. C., and Fersht, A. R. (2010) The tumor suppressor p53: from structures to drug discovery. *Cold Spring Harb. Perspect. Biol. 2*, a000919.

(15) Bell, S., Klein, C., Muller, L., Hansen, S., and Buchner, J. (2002) p53 contains large unstructured regions in its native state. *J. Mol. Biol. 322*, 917−927.

(16) Dawson, R., Muller, L., Dehner, A., Klein, C., Kessler, H., and Buchner, J. (2003) The N-terminal domain of p53 is natively unfolded. *J. Mol. Biol. 332*, 1131−1141.

(17) Yao, H. W., Xu, L. J., Feng, Y. G., Liu, D. S., Chen, Y. Y., and Wang, J. F. (2009) Structure-function correlation of human programmed cell death 5 protein. *Arch. Biochem. Biophys. 486*, 141−149.

(18) Liu, D. S., Feng, Y. G., Cheng, Y., and Wang, J. F. (2004) Human programmed cell death 5 protein has a helical-core and two dissociated structural regions. *Biochem. Biophys. Res. Commun. 318*, 391−396.

(19) Liu, D. S., Yao, H. W., Chen, Y. Y., Feng, Y. G., Chen, Y. Y., and Wang, J. F. (2005) The N-terminal 26-residue fragment of human programmed cell death 5 protein can form a stable alpha-helix having unique electrostatic potential character. *Biochem. J. 392*, 47−54.

(20) Cheng, Y., and Patel, D. J. (2004) An efficient system for small protein expression and refolding. *Biochem. Biophys. Res. Commun. 317*, 401−405.

(21) Hagn, F., Klein, C., Demmer, O., Marchenko, N., Vaseva, A., Moll, U. M., and Kessler, H. (2010) BclxL changes conformation upon binding to wild-type but not mutant p53 DNA binding domain. *J. Biol. Chem. 285*, 3439−3450.

(22) Johnson, B. A., and Blevins, R. A. (1994) NMRView - a computer program for the visualization and analysis of NMR data. *J. Biomol. NMR 4*, 603−614.
(23) Markley, J. L., Bax, A., Arata, Y., Hilbers, C. W., Kaptein, R., Sykes, B. D., Wright, P. E., and Wuthrich, K. (1998) Recommendations for the presentation of NMR structures of proteins and nucleic acids - (IUPAC Recommendations 1998). *Pure Appl. Chem. 70*, 117−142.
(24) Fielding, L. (2007) NMR methods for the determination of protein-ligand dissociation constants. *Prog. Nucl. Magn. Reson. Spectrosc. 51*, 219−242.
(25) Lee, C. W., Sorensen, T. S., Shikama, N., and La Thangue, N. B. (1998) Functional interplay between p53 and E2F through co-activator p300. *Oncogene 16*, 2695−2710.
(26) Lee, H., Mok, K. H., Muhandiram, R., Park, K. H., Suk, J. E., Kim, D. H., Chang, J., Sung, Y. C., Choi, K. Y., and Han, K. H. (2000) Local structural elements in the mostly unstructured transcriptional activation domain of human p53. *J. Biol. Chem. 275*, 29426−29432.
(27) Tang, C., Ghirlando, R., and Clore, G. M. (2008) Visualization of transient ultra-weak protein self-association in solution using paramagnetic relaxation enhancement. *J. Am. Chem. Soc. 130*, 4048−4056.
(28) Chipuk, J. E., Maurer, U., Green, D. R., and Schuler, M. (2003) Pharmacologic activation of p53 elicits Bax-dependent apoptosis in the absence of transcription. *Cancer Cell 4*, 371−381.
(29) Meek, D. W., and Anderson, C. W. (2009) Posttranslational modification of p53: cooperative integrators of function. *Cold Spring Harb. Perspect. Biol. 1*, a000950.